Tikrit Journal of Engineering Sciences (2024); 31(4): 202-221
DOI: http://doi.org/10.25130/tjes.31.4.20

IRAQI Academic Scientific Journals

ISSN: 1813-162X (Print); 2312-7589 (Online)
Tikrit Journal of Engineering Sciences
available online at: http://www.tj-es.com

TJES Tikrit Journal of Engineering Sciences

The Impact Load Behavior of Reinforced Concrete Slab Samples Containing Waste Plastic Aggregate

Suhaib Yahya Kasim AL-Darzi [a], *Kaythar A. Ibrahim* [*b], *Oday Asal Salih* [a]

a Civil Engineering Department, College of Engineering, University of Mosul, Mosul, Iraq.
b Environmental Engineering Department, College of Engineering, University of Mosul, Mosul, Iraq.

Keywords:
Shredded plastic; Sustainable concrete; Impact load; PET; Finite element.

Highlights:

- *Different percentage of recycled PET used in RC slabs.*
- *RC slab with PET experimentally tested by impact load and analyzed by FE.*
- *Response of PET's slab to impact was described.*

ARTICLE INFO

Article history:

Received	16 June	2023
Received in revised form	14 Oct.	2023
Accepted	01 Dec.	2023
Final Proofreading	01 Mar.	2024
Available online	23 Dec.	2024

Citation: AL-Darzi SYK, Ibrahim KA, Salih OA. **The Impact Load Behavior of Reinforced Concrete Slab Samples Containing Waste Plastic Aggregate**. *Tikrit Journal of Engineering Sciences* 2024; **31**(4): 202-221.
http://doi.org/10.25130/tjes.31.4.20

*Corresponding author:

Kaythar A. Ibrahim
Environmental Engineering Department, College of Engineering, University of Mosul, Mosul, Iraq.

Abstract: In the present study, eight reinforced concrete slabs divided into four groups with two slabs per group were fabricated and tested under impact load, replacing their aggregate with 0%, 4%, 8%, and 16% of polyethylene terephthalate (PET). During the preparation process, PET materials increased the workability of fresh concrete by up to 16% and decreased the density by 9%. The compressive strength decreased by about 11.7%, 15.7%, and 19.9% using 4%, 8%, and 16% of PET, respectively. Splitting strength decreased by 7.2%, 17.4%, and 20.3% using 4%, 8%, and 16% of PET, respectively. Failure mode and deflection amplitude results showed that PET delayed the first cracks and reduced the crack lengths and width and crack spreading at failure. Also, impact resistance enhanced at the first crack and ultimate load stages when PET was used compared to normal concrete. The maximal and minimal displacement decreased with increasing PET proportion to 8% and 16%. The slabs were modeled using the finite element program SAP2000 with 4-node shell elements. The finite element (FE) analysis showed a similar deflection response as those experimentally obtained for all slabs. The deflection obtained by FE was less, about 15.5% and 19%, compared with all slabs experimentally tested except slab G2-2, which showed a higher deflection of about 16.3%.

سلوك الحمل التصادمي لنماذج بلاطة خرسانية مسلحة محتوية على ركام نفايات البلاستيك

صهيب يحيى قاسم [١]، قيثار عبد الوهاب إبراهيم [٢]، عدي عسل صالح [١]
[١] قسم الهندسة المدنية/ كلية الهندسة / جامعة الموصل / الموصل – العراق.
[٢] قسم هندسة البيئة/ كلية الهندسة / جامعة الموصل / الموصل – العراق.

الخلاصة
في هذه الدراسة، تم تصنيع ثمانية بلاطات خرسانية مسلحة مقسمة إلى أربع مجموعات تحتوي كل مجموعة على بلاطتين وتم اختبارها تحت تأثير الحمل التصادمي، تم استبدال الركام بنسبة ٠٪ ، ٤٪ ، ٨٪ ، و ١٦٪ من البولي إيثيلين تيرفثالات (PET). اثناء عملية تهيئة النماذج لوحظ ان اضافة PET تزيد من قابلية تشغيل الخرسانة الطازجة بنسبة تصل إلى ١٦٪ وتقلل الكثافة بنسبة ٩٪. كما ان مقاومة الانضغاط انخفضت بحوالي ١١,٧٪ و ١٥,٧٪ و ١٩,٩٪ باستخدام ٤٪ و ٨٪ و ١٦٪ من PET على التوالي وان مقاومة الانفلاق انخفضت بنسبة ٧,٢٪ و ١٧,٤٪ و ٢٠,٣٪ باستخدام ٤٪ و ٨٪ و ١٦٪ من PET على التوالي. أظهرت نتائج نمط الفشل والأود أن استخدام PET يؤخر ظهور الشقوق الأولى ويقلل من اطوال وعرض الشقوق وانتشار الشقوق عند الفشل. تم تسجيل تعزيز لمقاومة الصدمات في مراحل حمل الشق الاول والحمل الاقصى عند استخدام PET مقارنة بالخرسانة العادية مع انخفاض الحد الأقصى والأدنى من الإزاحة عند زيادة نسبة PET إلى ٨٪ و ١٦٪. تم نمذجة البلاطات باستخدام برنامج SAP2000 باستخدام عناصر محددة قشرية ذات ٤ عقد. أعطى تحليل طريقة العناصر المحددة FE استجابة اود مماثلة لتلك التي تم الحصول عليها عمليا لجميع البلاطات. كما لوحظ ان قيمة الاود الذي تم الحصول عليه بواسطة FE أقل بحوالي ١٥,٥٪ و ١٩٪ ، مقارنة بجميع البلاطات التي تم فحصها عمليا باستثناء اللوح G2-2 ، والذي أعطى انحراف أعلى بحوالي ١٦,٣٪.

الكلمات الدالة: البلاستيك الممزق، الخرسانة المستدامة، حمل التأثير، البولي إيثيلين تيرفثالات، العناصر المحدودة.

1.INTRODUCTION

Typically, reinforced concrete construction was made to withstand static load forces. Even though an impact load is an unintended load that could influence the structure, it should still be considered [1,2]. Impact forces from various sources, such as industrial accidents, automobile collisions, rock falls, and even acts of war, could harm the reinforced concrete slab. Thus, it is intriguing to study reinforced concrete slabs' responses to impact loads [3,4]. Even though research had primarily concentrated on analyzing and designing against high-velocity hits like those from ballistic missiles, the impact behavior of the reinforced concrete slab had also been the subject of an extensive experimental study using low-velocity impacts [5,6]. Several kinds of research were conducted using finite element analysis and other computational and experimental methods to determine how local impacts affect the reinforced concrete slabs [7–9]. At the same time, recycling water bottle plastic (polyethylene terephthalate, or PET) is a major contributor to the worldwide problem of solid waste. Using recycled materials to make concrete has been considered a way to save money, improve quality, and protect the environment [10,11]. Several studies have investigated whether or not it would be possible to use recycled plastic in concrete instead of burying plastics [12-14]. Researchers usually studied the material's density, porosity, compressive and flexural behavior, and permeability to see if they changed when plastic was introduced [15,16]. Saxena et al. [17] studied PET bottles as fine and coarse aggregate in concrete at different replacement percentages: 5%, 10%, 15%, and 20% by weight of concrete. The test analysis findings showed decreasing in compressive strength when using PET. However, compared to control concrete, the results showed that plastic concrete had better resilience to impact loading. Hama [18] studied using plastic water bottle caps (CPPA) as a partial replacement for coarse aggregates in concrete. The results indicated that strengths increased for plastic content between 15% and 30%, particularly at 15%, and dropped as plastic content was raised over 30%. With a 45% increase in plastic content, more blows in R.C. slabs failed. The investigation's findings suggested using between 15% and 30% of this kind of plastic as a partial replacement for gravel in structural R.C. Hashim et al. [19] examined the low-velocity impact resistance of composite steel plate-concrete slabs under various volume fractions of plastic fiber. According to test results, adding plastic fibers to concrete greatly increased the ability to withstand impacts. A change in fiber content from 0.5 to 0.75% was observed to result in a marginal gain in energy absorption. Glass and plastic wastes were combined with concrete by Mohammed and Hama [20] to create green concrete in 2022. The cement was partially replaced with waste glass powder, while the fine aggregates were partially replaced with crushed waste plastic. According to the findings, concrete's characteristics were enhanced by adding glass alone. However, when 15% glass powder was used instead of sand, it negatively impacted the concrete's compressive strength, splitting tensile strength, flexural strength, elastic modulus, and bond strength. On the other hand, 431.57% for 20% plastic aggregate has demonstrated the energy absorption capacity under impact load. High-strength concrete that incorporated waste fiber of PET was tested for its mechanical properties, first cracking, and ultimate load impact by Mohammed and Karim [21]. As a result of adding PET fiber, they were lowered. Fiber

content increased flexural strengths and splitting tensile, regardless of fiber length and fraction volume. Depending on the fraction volume and fiber length, improvements in the first crack impact have been documented up to 300% and for ultimate load impact up to 833%. Smaoui et al. [22] examined PET strip-shaped inclusions' impact on concrete performance using PET fractions up to 20 kg/m3. It has been demonstrated that the heat treatment increased the inclusions' tensile strength to 120%. Therefore, the concrete's mechanical qualities significantly improved. Investigations were extended to study blast waves and ballistic impacts. The findings showed better protection against the threat of explosive and bullet attacks. Hama et al. [23] studied the influence of adding waste ring plastic fibers (WRPF) to concrete and how it would react to compression, tensile, bending, and impact loads. The findings indicated that for tiny fiber fractions, introducing fibers improved the behavior of concrete specimens subjected to compression force. The best impact resistance under the impact load was 1% WRPF. According to the review of the literature, there is still a need for more research to understand the full behavior of RC with recycled PET under impact load. In addition, this study aims to investigate the effect of impact load on RC slab using local concrete composition materials with PET recycled plastic and study the displacement response over time under the impact load effect. To the author's knowledge, no simulation of the experimental impact load slab test can be used to study more different cases and behavior of structures under the impact load effect. Therefore, this study focuses on this simulation using the finite element method. This study aims to investigate the effects of impact loads on a reinforced concrete slab made with PET recycled plastic, as shown in Chart 1.

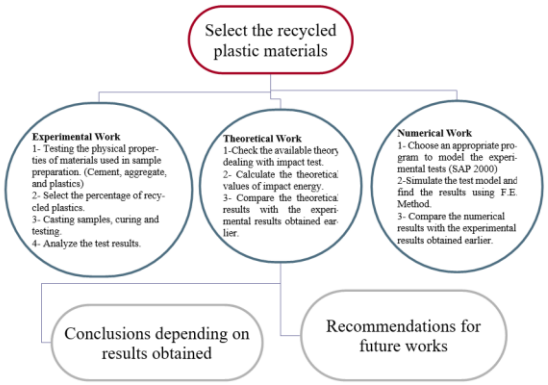

Chart 1 Flow-Chart of Working Methodology.

The main goal of the present work is to investigate the effect of using plastic as a partial replacement of aggregate on the mechanical properties, strength, and damping of the reinforced concrete slab by conducting the following:

- Fabricate and experimentally test standard concrete cylinders for compressive and splitting. The tests investigated the PET effect on the concrete's mechanical properties.
- Casting, curing, and experimentally testing eight reinforced concrete slab samples to investigate the effect of using concrete with PET on the impact resistance. Accordingly, the mode of failure, cracks, deflection amplitude with time, and impact energy of the concrete slab samples were investigated.
- Use the SAP program to investigate the possibility of simulating the experimental impact slab test to verify the of th FE method's accuracy in simulating such a test.

2.EXPERIMENTAL WORK MATERIALS AND METHODS

A concrete mixture proportion of (1: 2.4: 3.35; cement: sand: gravel, and w/c=0.4) by weight was selected to investigate the concrete's mechanical properties. The aggregate was replaced by (0% to 4%, 8%, and 16%) weighting proportions of PET. Locally available cement that met the Iraqi specification (No.5/2019) was used, as shown in Table 1 [24].

Table 1 Physical and Chemical Properties of the Cement.

Physical Characteristics	Specification	Value	Units
Standard Consistency w/c	----	0.285	-
Initial setting	≥ 45	100	Minutes
Final setting	≤ 600	240	Minutes
Compressive strength (3 days)	≥ 15	23.6	MPa
Compressive strength (7 days)	≥ 23	33.7	MPa
Fineness (sieve no. 170)	≤ 10	5.0	%
Chemical Components	**Specification (IQS:5/2019)**	**Value**	**Units**
SiO_2	-	21.26	%
Fe_2O_3	-	3.6	%
AL_2O_3	-	4.2	%
CaO	-	60.2	%
SO_3	≤ 2.5	2.31	%
MgO	≤ 5	2.75	%
Free Lime	-	1.23	%
Insoluble residue	≤ 1.5	0.7	%
Loss on ignition	≤ 4	2.94	%
Total	-	99.72	%
Solid Solution	-	16.06	%

Sand meeting (IQS) No. 45/1984 specification zone 2 [25], as shown in Table 2 and Fig. 1, was used. The coarse aggregate with a maximum size of 5-14mm also complied with the Iraqi Specification (No. 45/1984) requirements, as shown in Table 3 [25]. The clear bottled water produced initially by the polyethylene terephthalate (PET) was recycled by a company in Mosul's commercial district to produce tiny sheets with an average size of 4 to 10 mm fibers used to replace the aggregate. The PET fibers' characteristics are described in Table 4. The

concrete materials and the recycled shredded waste plastic PET used in the study are shown in Fig. 2. Potable water was used for concrete mixing and curing [26]. An 8mm diameter deformed steel reinforcement bars were placed in two orthogonal directions in each slab. The rebar was tested according to ASTM A615/A615M–15 [27] and gave a yield strength of (423.8MPa) and ultimate strength of (637.6MPa) [27], as shown in Table 5.

Table 2 Properties of Fine Aggregate Zone 2.

Sieve Size (mm)	Passing %	Passing% Limits (IQS:45/1984)
10	**100**	**100**
4.75	93	90 – 100
2.36	80	75 – 100
1.18	64	55 – 90
0.6	48	35 – 59
0.3	15	8 – 30
0.15	4	0 – 10
Specific Gravity	2.64	
Fineness Modulus	2.96	

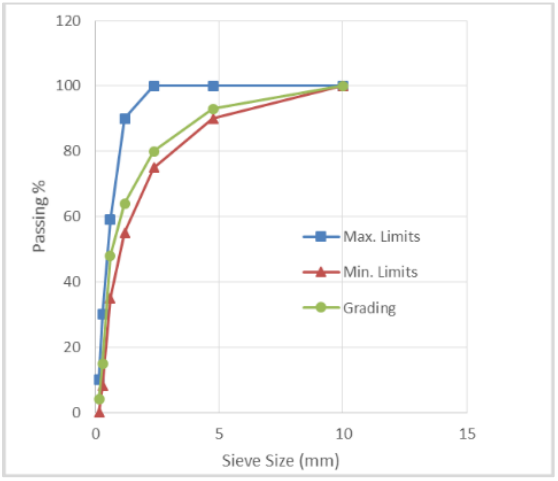

(a) Sieve Analysis of Sand.

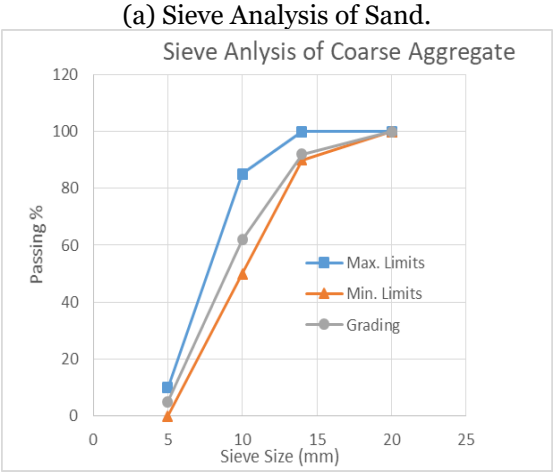

(b) Sieve Analysis of Coarse Aggregate.

Fig. 1 Sand and Coarse Aggregate Sieve Analysis and Limits.

Table 3 Properties of Coarse Aggregate with Maximum Aggregate Size 5-14mm.

Sieve Size (mm)	Passing %	Passing% Limits (IQS:45/1984)
20	100	100
14	92	90 – 100
10	62	50 – 85
5	5	0 – 10
Specific Gravity	2.68	

(a) Slab Shuttering and Reinforcement.

(b) Sand Materials.

(c) Gravel (Coarse Aggregate).

(d) PET Materials.

Fig. 2 Slab Shuttering, Aggregate, and PET Materials.

Table 5 Reinforcement Steel Bars Testing Results.

Bar Diameter (mm)	Value	Specification ASTM A615
Ultimate Strength (MPa)	637.6	>620
Yield Stress (MPa)	423.8	>420
Elongation %	24	>9%

The control mix was designed with a moderate slump to achieve the targeted theoretical compressive strength of 28 MPa at 28 days [28]. Four concrete mixtures were cast with the proportions shown in Table 6. Each concrete batch's density was measured according to the ASTM- C138 standard, as shown in Table 6 [29, 30]. Slump tests were performed for the fresh concrete of each concrete mixture, and the slump measurement results are listed in Table7.

Table 4 Physical Properties of PET Plastic.

Type	Shape	Density (gm/cm3)	Color	Aspect ratio (L/d)	Width (mm)	Thickness (mm)
PET	Rectangular	1.35	Transparent	1 to 2.5	4 to 10	0.3

Four standard cylinders for each concrete mixture, having a diameter of 150mm and a length of 300mm, were cast and cured in a water basin [30]. Three cylinders were tested for compression, and one cylinder was tested for each group for splitting [31,32]. The cylinder test results are shown in Table 7 and Fig. 3. The adopted mixes were used simultaneously to cast identical sets of slab samples with dimensions of (450x450x100mm). These slabs were divided into four groups, with two slabs for each group. The names and descriptions of the four groups are listed in Table 8. All experiments on hardened concrete were performed when the concrete had aged for 28 days in the material laboratory of the College of Engineering at the University of Mosul. Figure 4 shows the instrument used to conduct impact testing. The slabs' samples were placed on a square base frame within four inclined arms fixed on a measuring cell connected to a sensitive data logger. The data logger recorded the displacements of each drop within a time step of 0.01 seconds. The steel ball had a 3 kg mass and was dropped by gravity at the slab's center after releasing it from the cantilever lever arm spaced 1.0m from the slab's top. The tests examined how the slab specimens would perform under impact by dropping the balls several times up to failure. The slab's response under each drop was recorded and saved to a computer by a data logger. The first cracks and breaking of the slab were identified and recorded during the test for each slab.

Table 6 Concrete Mixing Proportion.

No	Group	Total Replacement %	Cement	Fine agg.	Coarse agg.	Water	%Replacement of fine aggregate	%Replacement of Coarse Aggregate	Density kg/m3
1	G1	0	1	2.40	3.35	0.40	0	0	2169
2	G2	4%	1	2.36	3.28	0.40	2	2	2115
3	G3	8%	1	2.31	3.22	0.40	4	4	2060
4	G4	16%	1	2.21	3.08	0.40	8	8	1967

Table 7 The Slump, Compressive Strength, and Splitting Strength of Cylinders Tests.

No.	Group	1st Cylinder Comp. Strength MPa	2nd Cylinder 2 Comp. Strength MPa	third Cylinder Comp. Strength MPa	Average Comp. Strength MPa	% diff. Comp. str.	Splitting Strength MPa	% diff. Splitting str.	Slump mm
1	G1	29.91	28.93	29.12	29.32	--	2.76	--	102
2	G2	25.32	26.24	26.12	25.89	-11.69	2.56	-7.17	108
3	G3	23.69	24.61	25.89	24.73	-15.65	2.28	-17.42	112
4	G4	22.98	23.65	23.86	23.50	-19.86	2.20	-20.29	118

(a) Compression Test. **(b)** Splitting Test.

Fig. 3 The Setup of the Cylinder for Compression and Splitting Test.

Table 8 Names and Description of the Slab Groups.

No.	Group Name	Description
1	G1	Control Slab Replacing 0.0%
2	G2	Replace 4% of aggregate by PET
3	G3	Replace 8% of aggregate by PET
4	G4	Replace 16% of aggregate by PET

(a) Impact Test Instruments and Data Logger.

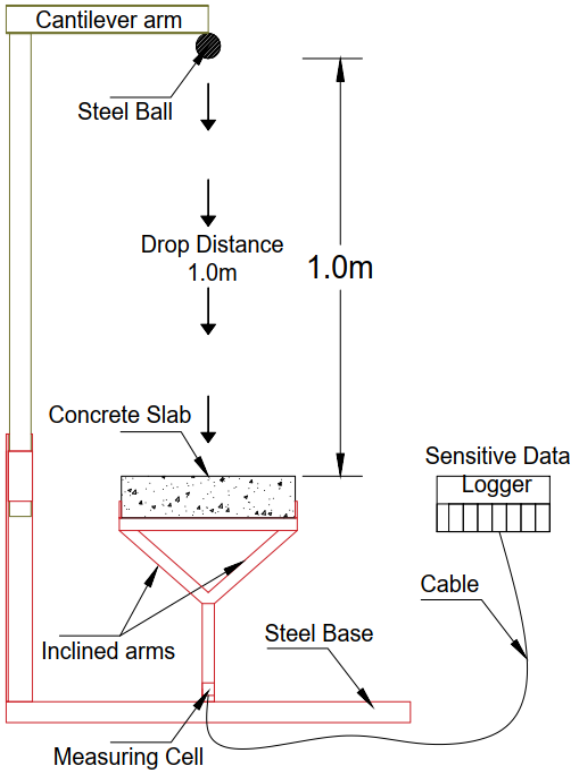

(b) Test Setup.

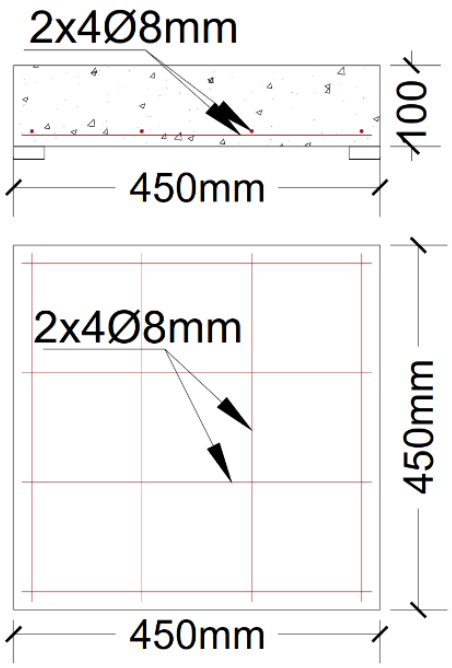

(c) Slab Dimensions and Reinforcement.

Fig. 4 Slab Details, Test Setup, and Impact Instruments Components.

The impact energy received by the slab due to dropping balls was estimated by Eq. (1) [33].

$$IE = \sum_i^n m_i . h_i \quad (1)$$

The ball falls due to gravity, and the speed of falling (v) will be;

$$v = (2.g.h)^{0.5} \quad (2)$$

The average impact force can be calculated (IF) as;

$$IF = 0.5 . m . v^2 \quad (3)$$

where mi is the drop ball weight (3.0 kg), hi is the dropping height (hi=1.0 m), i is the number of drops, n is the total number of blows, IE is the impact energy (N.m), and g is the acceleration due to gravity (9.8m/s) [34]. The above equations yielded the same results as those obtained by Saxena [17].

3.EXPERIMENTAL TEST RESULTS AND DISCUSSION

3.1.Effect of PET on Concrete Mechanical Properties

As shown in Table 6, PET in concrete reduced the density by 2.5% to 9.3%. Meanwhile, Table 7 shows that the workability increased when PET was used in the concrete matrix since the slump increased by about 6% to 16% compared to normal concrete. The cylinders' compressive strength obtained for the four groups listed in Table 7 showed that replacing aggregate with PET decreased the compressive strength compared to normal concrete (G1) by 11.69%, 15.65 %, and 19.86 % for G2, G3, and G4, respectively. The reduction in compressive strength was due to the poor bonding between the PET and other concrete materials, which was the same result of [14, 17, 35].

3.2.Effect of PET on Concrete Slab Behavior Under Impact Loads

The impact test was conducted by dropping the ball multiple times and recording the slab response after each drop. The process was repeated until the slab exhibited an almost consistent response. The slab surface was crushed in the early stages, and cracks appeared from the slab's center. With repeating the ball's drop, the cracks developed, increased, and became wider up to failure, as shown in Fig. 5, for the four groups. The control slab cracks (Group G1) formed in a branching pattern, with wider cracks, and had the most extended cracks compared to the other groups. Also, the crack widths in groups G2 and G3 were more significant than in G4. The impact energy calculated using Eq. (1) is listed in Table 9. Table 9 shows the number of drops employed for each group and the impact energy of the slabs based on the test findings at the first crack and at failure. Slabs in groups G2, G3, and G4 containing PET outperformed the control group G1 regarding impact resistance at first fracture and ultimate failure. Groups G2 and G3 required more blows than control group G1 before the first crack appeared, and the specimens failed. Based on the findings, the first cracks appeared earlier if PET was absent from the concrete mix. Compared to the control group, the number of drops that caused slab failure increased by increasing the percentages of PET. Finally, the group G4 specimens, which contained the highest percentage of PET, required more blows than the other groups before the first crack appeared, and the specimens ultimately failed. The impact resistance of the PET material group steadily improved when the amount of PET in the mix was increased [17, 19, 20, 23]. The micro-cracks were likely bridged due to the large number of shredded plastic fibers added to the concrete slabs, which greatly enhanced PET's internal binding strength and, hence, the concrete's internal energy (impact resistance). The reasons for this behavior include the fiber's excellent resistance to impact [19]. Figure 6 shows the displacement recorded for the slab with time subjected to impact due to the balls' drop. The maximal and minimal displacement amplitudes of the slabs are shown in Table 10. Figures 7 and 8 show midspan maximum and minimum amplitude displacement as it interacts with the drops. The results showed that the maximum displacement amplitude decreased with increasing the PET ratio for all groups except G2 (drops 23 and 24) and G3 (in a sporadic fashion) while decreasing more predictably for the G4 groups. It had a minimum amplitude of displacement than group G1. The final phases showed more irregular changes for groups G2 and G3 than for group G1. A possible explanation is that fiber interacts with the concrete distinctively. Figure 9 shows the percentage differences in maximum displacement recorded by groups G2, G3, and G4 compared to the control group's G1. Figure 10 demonstrates the differences in minimum displacement obtained from adding PET to concrete in groups G2, G3, and G4 compared to the control group G1. It can be seen clearly that the maximum displacement amplitudes differed by 29.7% to -29.5% between groups G2 and G1, 12.5% to -50.5% between groups G3 and G2, and 33.7% to -10.6% between groups G4 and G1. Minimum displacement amplitude differences ranged from 0% in group G2 to -33.7% in group G1, 10.4% in group G3 to -39.4% in group G4, and 13.1% to -19.8% in group G4.

Table 9 Slab Test Impact Energy Results.

No.	Group	% Replacement	No. of blows at 1st crack	No. of blows at failure	Impact Energy at 1st crack N.m	Impact Energy at failure N.m
1	G1	0.0%	3	22	90	660
2	G2	4 % PET	4	25	120	750
3	G3	8 % PET	4	25	120	750
4	G4	16 % PET	5	26	150	780

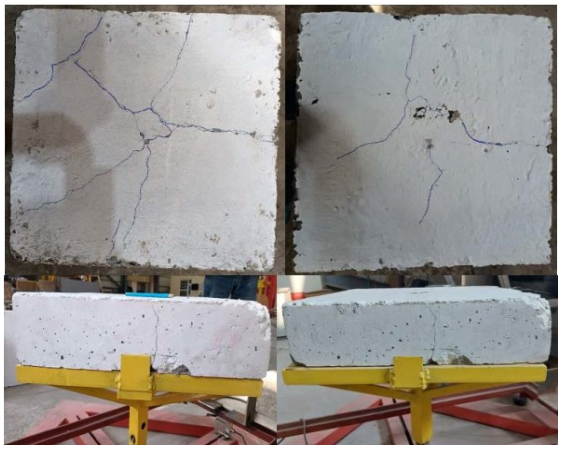

(a) Control Slab 0.0% (G1).

(b) 4% PET Replacement (G2).

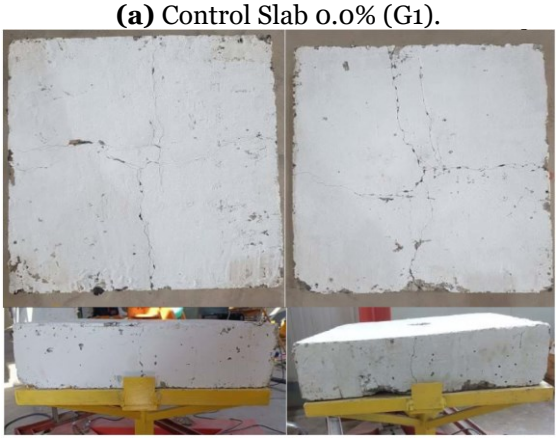

(c) 8% PET Replacement (G3).

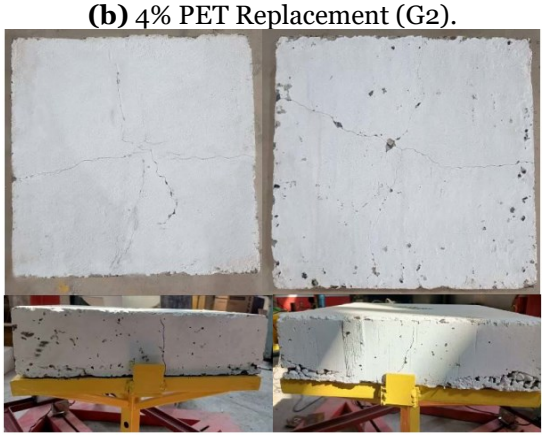

(d) 16% PET Replacement (G4).

Fig. 5 The Failure Shape of the Tested Slabs.

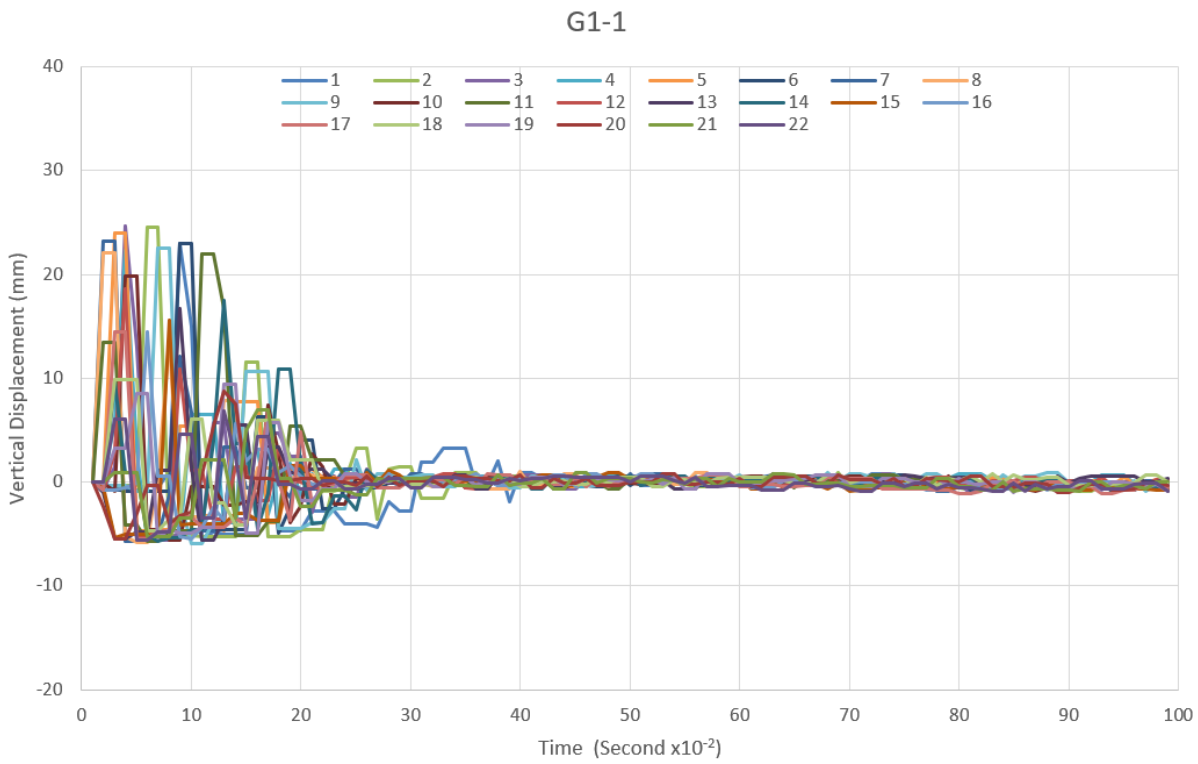

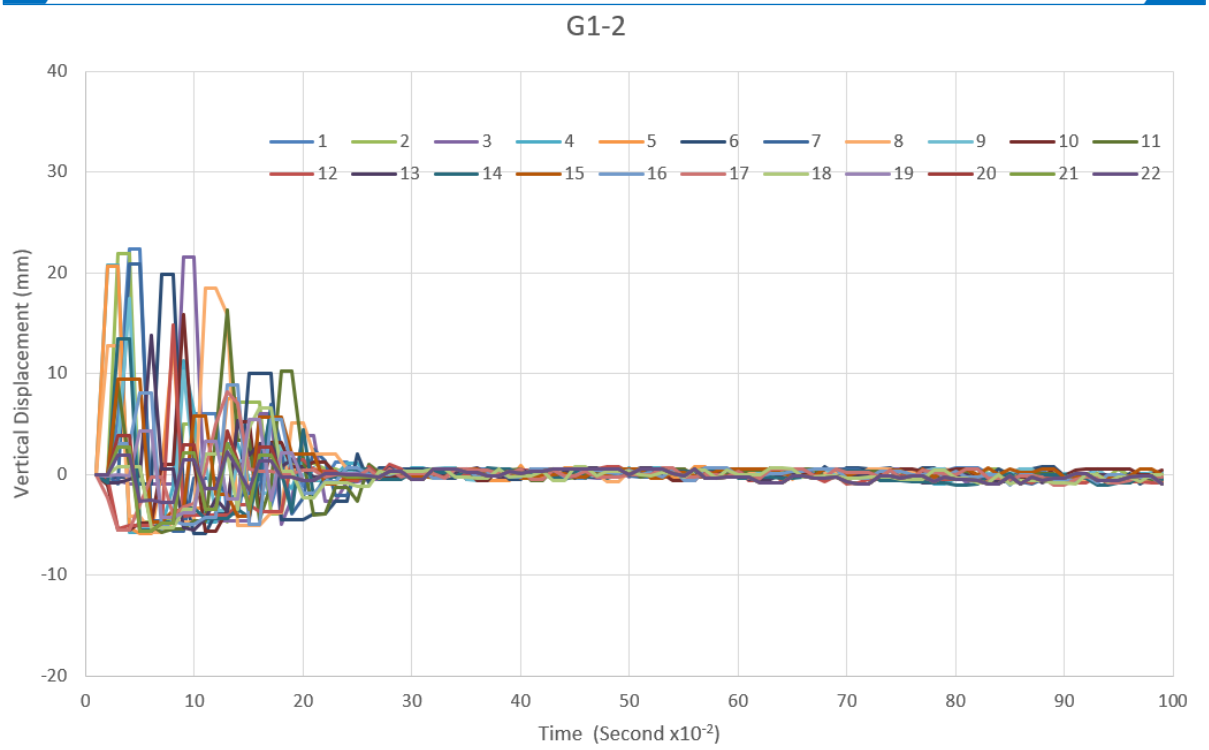
G1-2
1 2 3 4 5 6 7 8 9 10 11
12 13 14 15 16 17 18 19 20 21 22
Vertical Displacement (mm)
40
30
20
10
0
-10
-20
0 10 20 30 40 50 60 70 80 90 100
Time (Second x10-2)

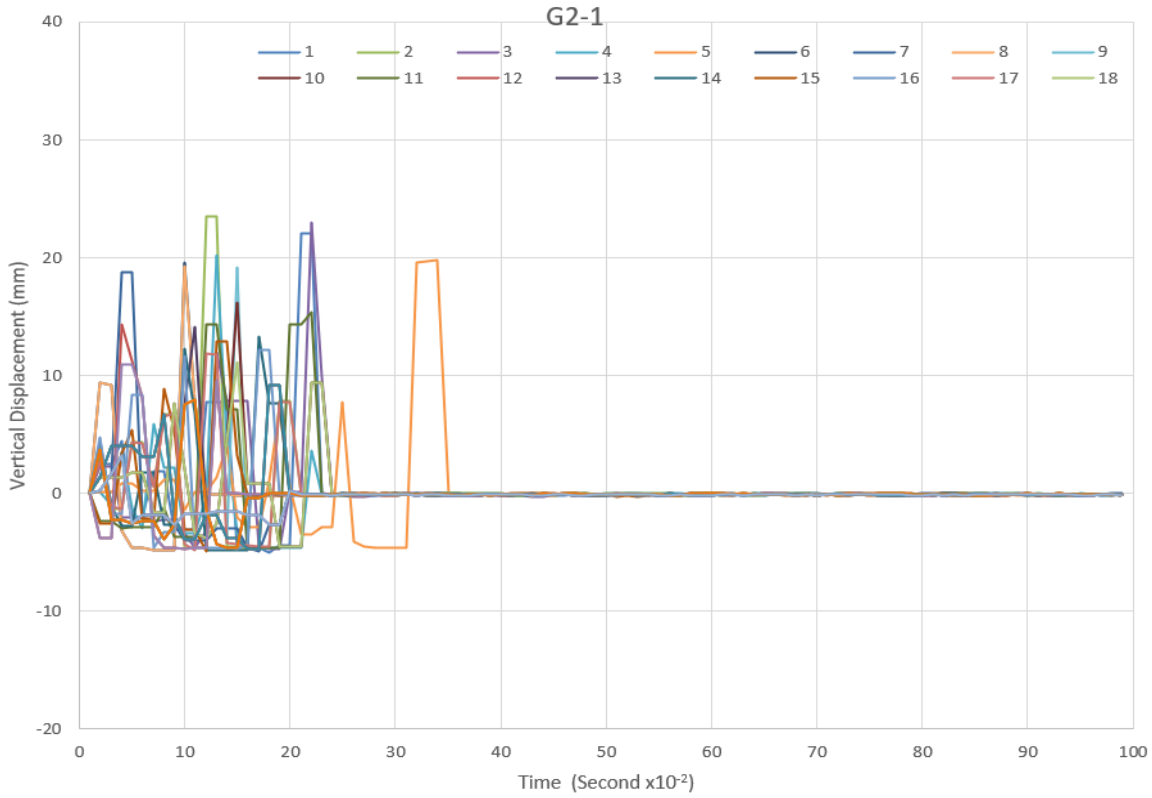
G2-1
1 2 3 4 5 6 7 8 9
10 11 12 13 14 15 16 17 18
Vertical Displacement (mm)
40
30
20
10
0
-10
-20
0 10 20 30 40 50 60 70 80 90 100
Time (Second x10-2)

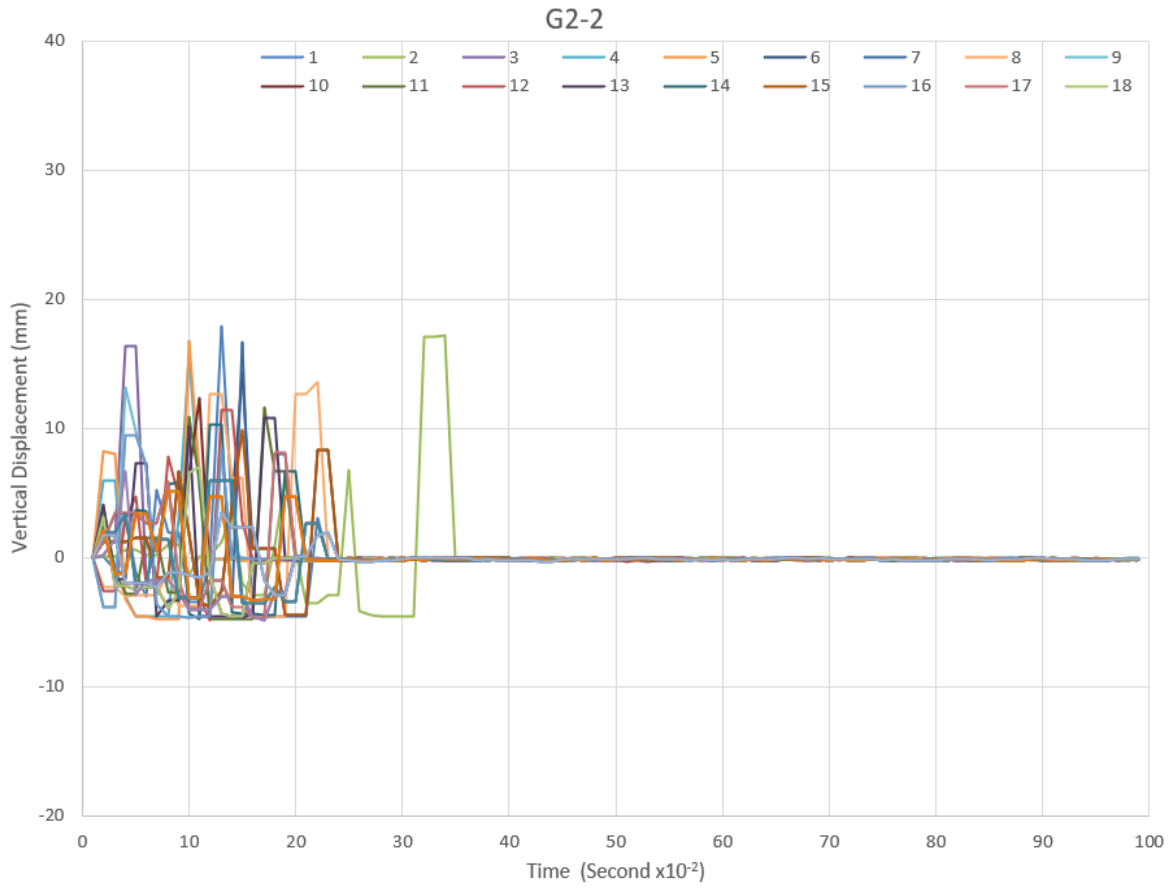
G2-2
1
2
3
4
5
6
7
8
9
10
11
12
13
14
15
16
17
18
Vertical Displacement (mm)
Time (Second x10-2)

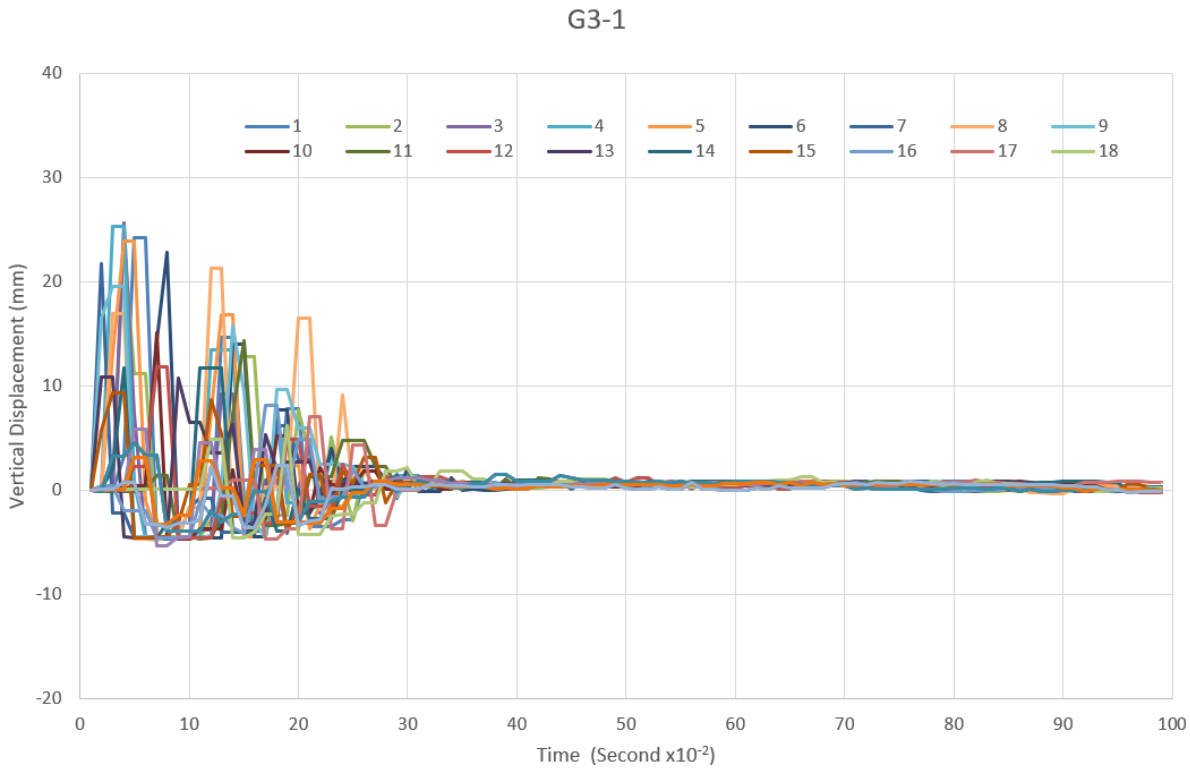
G3-1
1
2
3
4
5
6
7
8
9
10
11
12
13
14
15
16
17
18
Vertical Displacement (mm)
Time (Second x10-2)

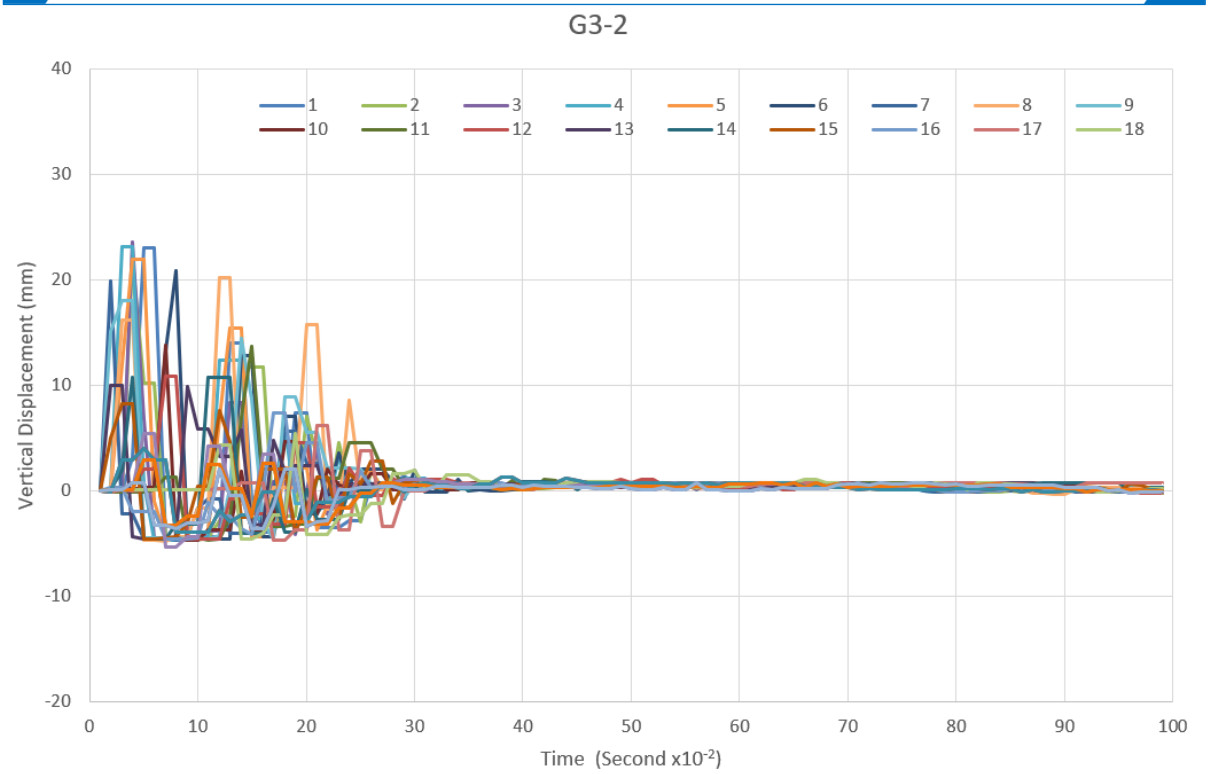
G3-2
1 2 3 4 5 6 7 8 9
10 11 12 13 14 15 16 17 18
Vertical Displacement (mm)
Time (Second x10-2)

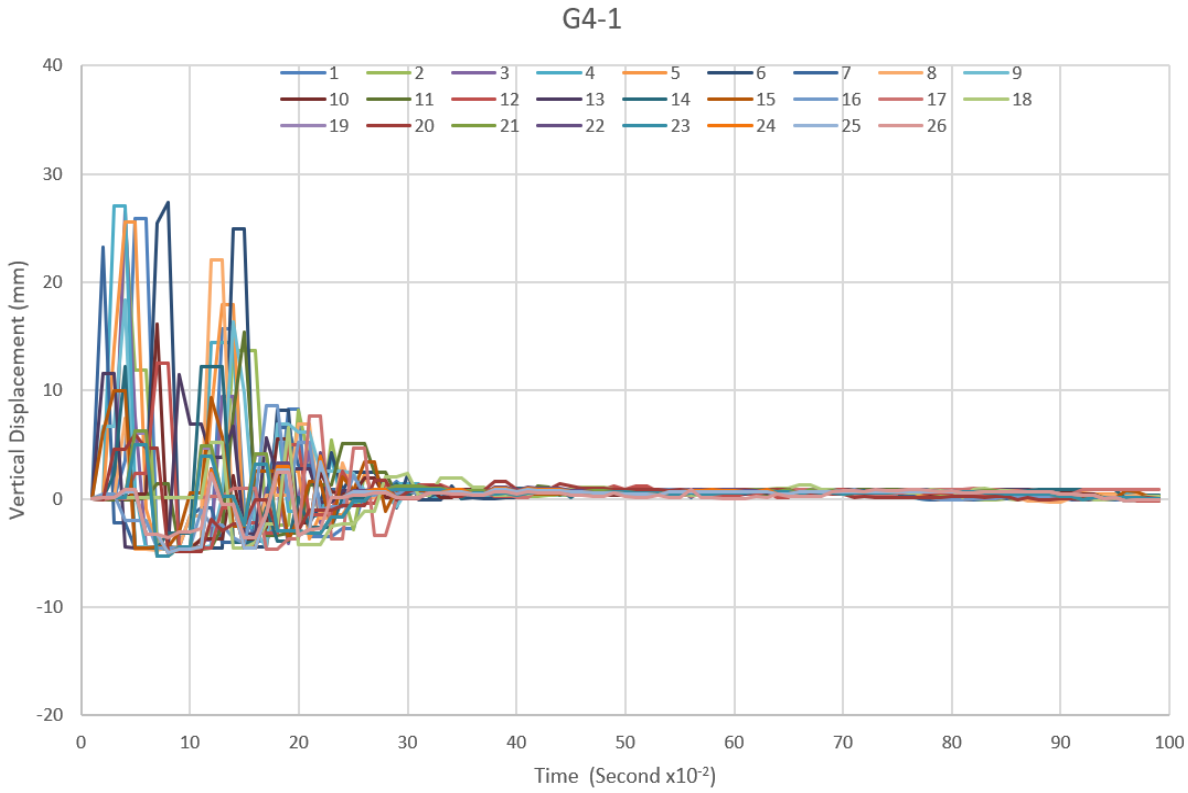
G4-1
1 2 3 4 5 6 7 8 9
10 11 12 13 14 15 16 17 18
19 20 21 22 23 24 25 26
Vertical Displacement (mm)
Time (Second x10-2)

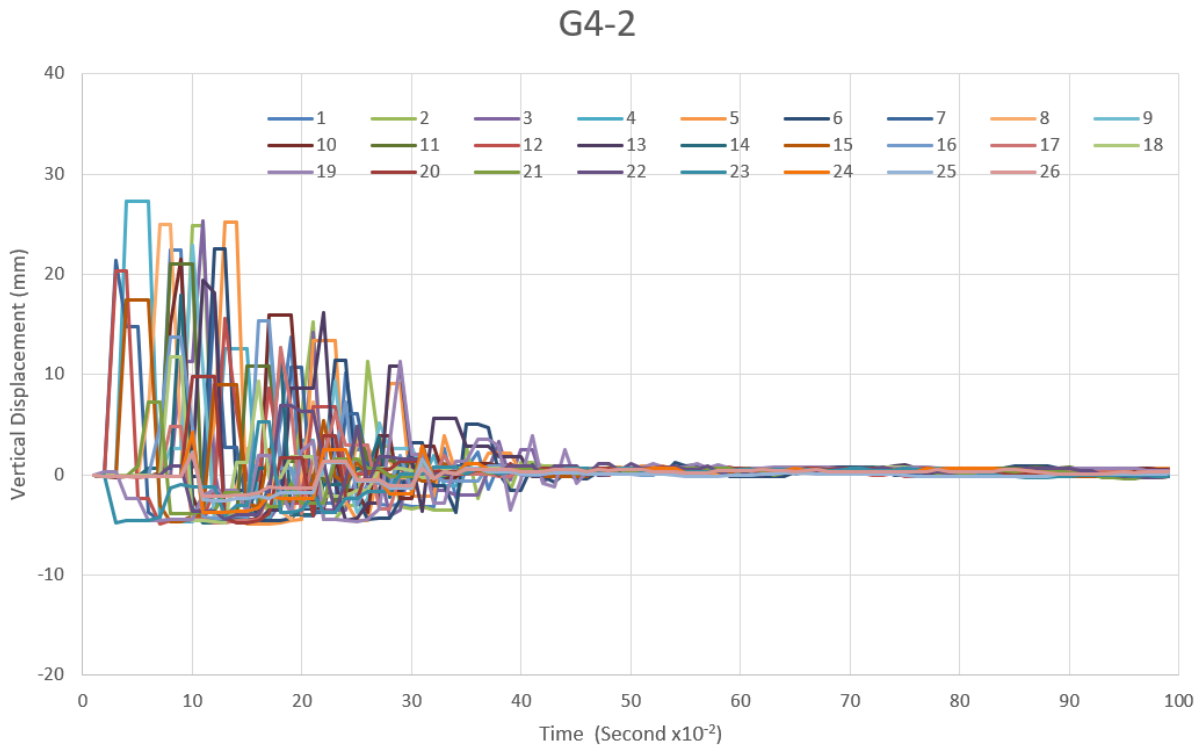

Fig. 6 The Displacement with Time for the Tested Slabs.

Table 10 Maximum and Minimum Amplitude of the Slabs Displacement Results.

Item	Experimental Results	Finite Element Results	% Differences
	G1-1	fc'=22 MPa	
Max. Displ. =	24.7	19.83	-19.72
Min. Displ.	-5.9	-11.03	86.95
	G1-2	fc'=22 Mpa	
Max. Displ. =	22.4	19.83	-11.47
Min. Displ.	-5.9	-11.03	86.95
	G2-1	fc'=25 Mpa	
Max. Displ. =	23.5	20.81	-11.45
Min. Displ.	-5	-11.5	130.00
	G2-2	fc'=25 Mpa	
Max. Displ. =	17.9	20.81	16.26
Min. Displ.	-4.9	-11.5	134.69
	G3-1	fc'=25 Mpa	
Max. Displ. =	25.7	20.81	-19.03
Min. Displ.	-5.3	-11.5	116.98
	G3-2	fc'=25 Mpa	
Max. Displ. =	23.6	20.81	-11.82
Min. Displ.	-5.3	-11.5	116.98
	G4-1	fc'=30 Mpa	
Max. Displ. =	27.4	22.09	-19.38
Min. Displ.	-5.3	-12.11	128.49
	G4-2	fc'=30 Mpa	
Max. Displ. =	27.3	22.09	-19.08
Min. Displ.	-4.9	-12.11	147.14

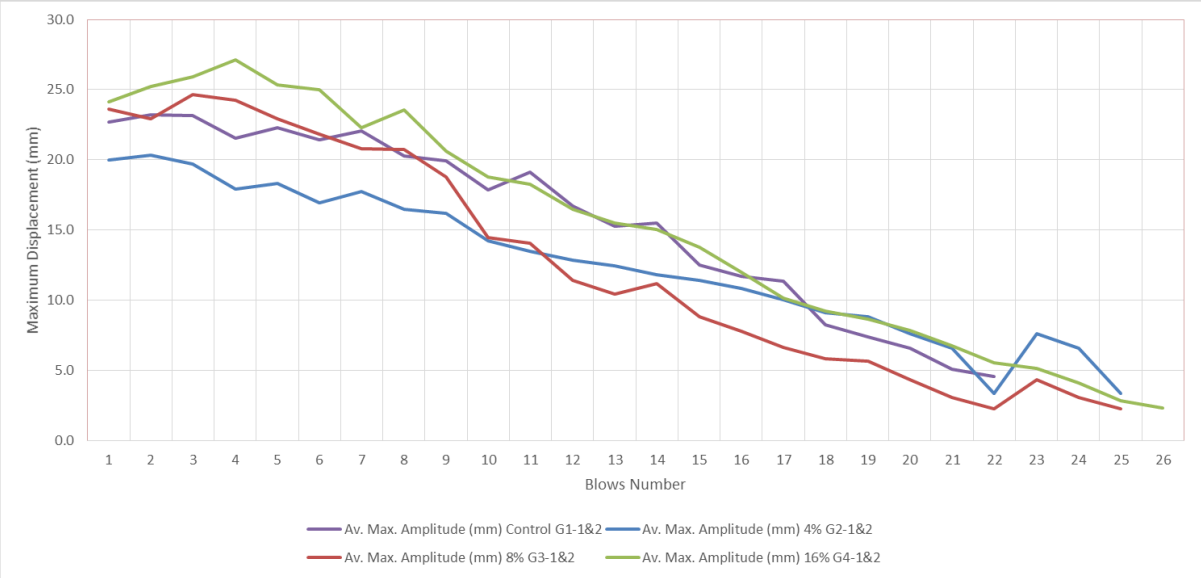

Fig. 7 The Maximum Displacement Amplitude for the Tested Slabs.

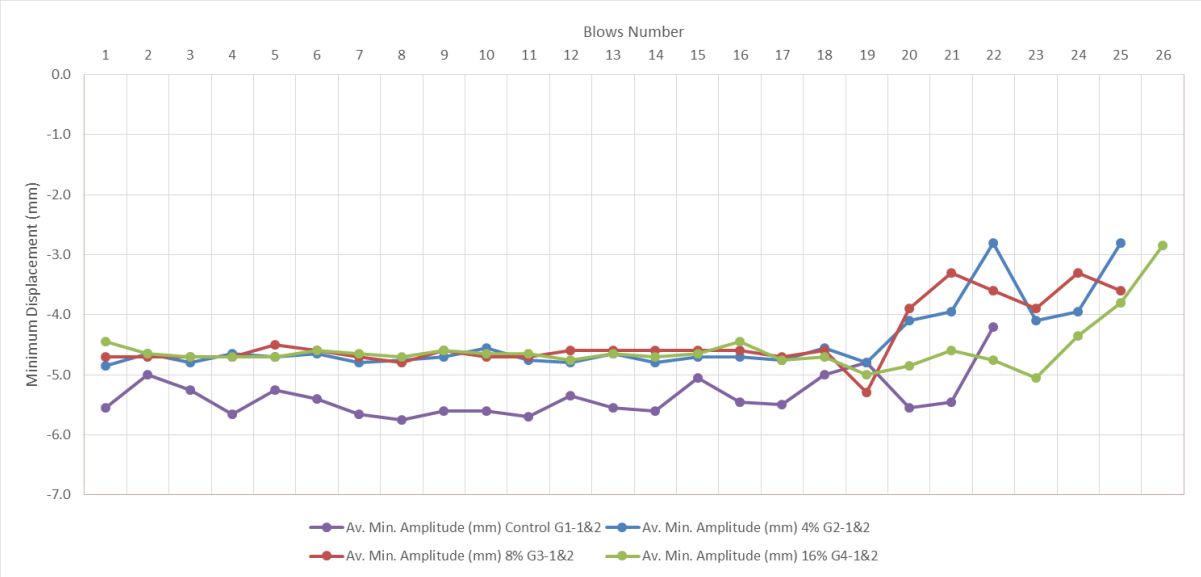

Fig. 8 The Minimum Displacement Amplitude for the Tested Slabs.

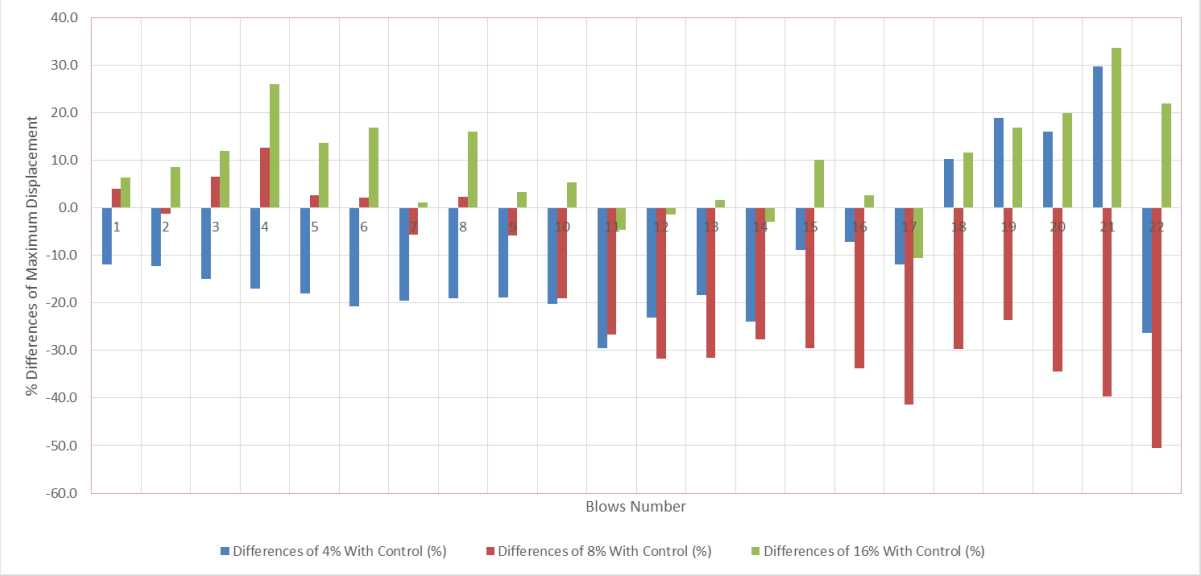

Fig. 9 The Differences of Maximum Displacement with Control Slabs.

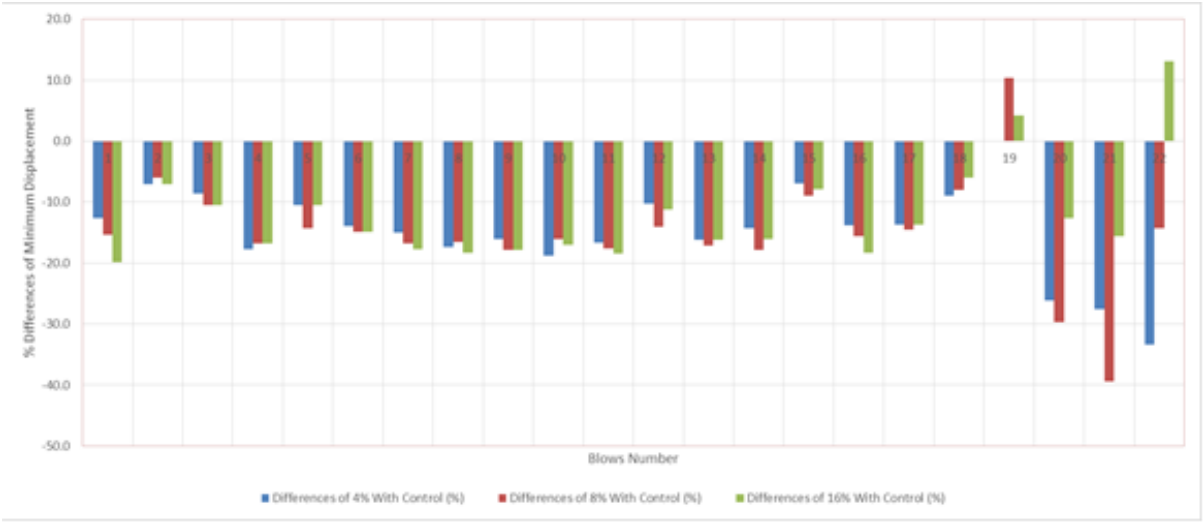

Fig. 10 The Differences of Minimum Displacement with Control Slabs.

4.FINITE ELEMENT ANALYSIS

4.1.Finite Element Modelling

The slab samples tested experimentally were modeled using the three-dimensional finite element program SAP2000 using four nodes of quadrilateral shell elements, as shown in Fig. 11. The shell element with three degrees of freedom (*u1, u2*, and *u3*) can simulate and compute strains (ε11, ε22, ε33, γ12, γ13, and γ23) from displacement and plate bending rotations, as presented in Eq. (4).

$$\begin{pmatrix} \varepsilon 11 \\ \varepsilon 22 \\ \varepsilon 33 \\ \gamma 12 \\ \gamma 13 \\ \gamma 23 \end{pmatrix} = \begin{pmatrix} \dfrac{du1}{dx1} \\ \dfrac{du2}{dx2} \\ \dfrac{du3}{dx3} \\ \dfrac{du1}{dx2} + \dfrac{du2}{dx1} \\ \dfrac{du1}{dx3} + \dfrac{du3}{dx1} \\ \dfrac{du2}{dx3} + \dfrac{du3}{dx2} \end{pmatrix} \quad (4)$$

where, u1, u2, and u3 are the translations in x1, x2, and x3 axes (or x, y, and z axes). Accordingly, the stresses (σ11, σ22, σ33, τ12, τ13, and τ23) contribute to all forces and plate-bending moments (normal forces, moments, and shear are calculated. A numerical integration formulation for stresses and internal forces calculation using 2×2 Gauss integration points was used and then extrapolated to the elements' joints [36–37]. Forty-six quadrilateral shell elements with 81 nodes were used to model the slab. The mesh size of the elements was 25×25mm in x and y directions to model the 400×400mm slab by considering the 2×25mm as support from all sides. The simple supporting constraints are assigned to nodes in X and Y planes, as shown in Fig. 11. An Impact Force (IF), i.e., calculated using Eqs. (1) - (3), was applied at the slab's middle joint, as shown in Fig. 11. The elastic finite element analysis was conducted using the modulus of elasticity calculated using the ACI-318 code Equation [38] and Poisson's ratio of 0.2.

4.2.Finite Element Results

The results of the displacement obtained from finite element analysis (FE) are shown in Fig. 12 for the control group (G1). The finite element models were also used to analyze three other models with different compressive strengths of (22, 25, 30, and 35 MPa). The results in terms of displacement with time at the midspan are shown in Fig. 13. The maximum and minimum displacements obtained with time from the finite element analysis are shown in Fig. 14 with time variation and listed in Table 10. The finite element results showed that the model adopted could handle the analysis and produce results like those experimentally obtained. The differences between the deflection showed a decrease in the deflection obtained by the finite element method of about 15.5% and 19% compared to groups G1, G3, and G4. The differences between finite element deflection and group G2 differed for sample G2-2. In contrast, a decrease in deflection of about 11.5% was obtained compared with G2-1, and an increase of about 16.3% was obtained compared with G2-2.

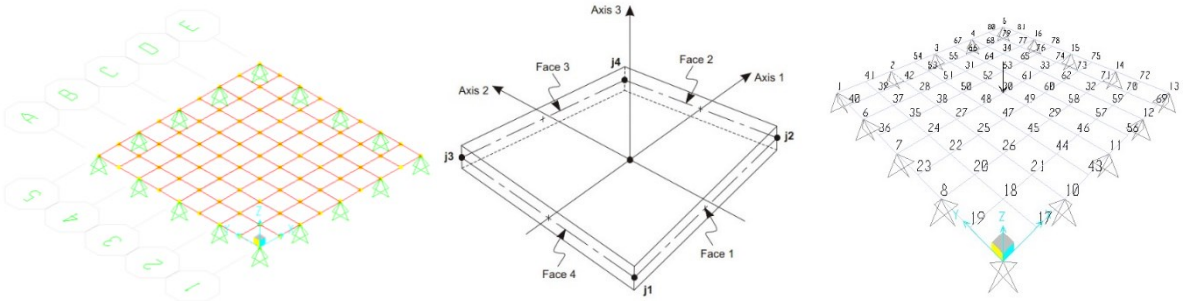

(a) Finite Element Meshing. **(b)** Quadilateral Shell Element. **(c)** Location of the Applied Vertical Load.

Fig. 11 Finite Element Mesh, Shell Properties, and Applied Load.

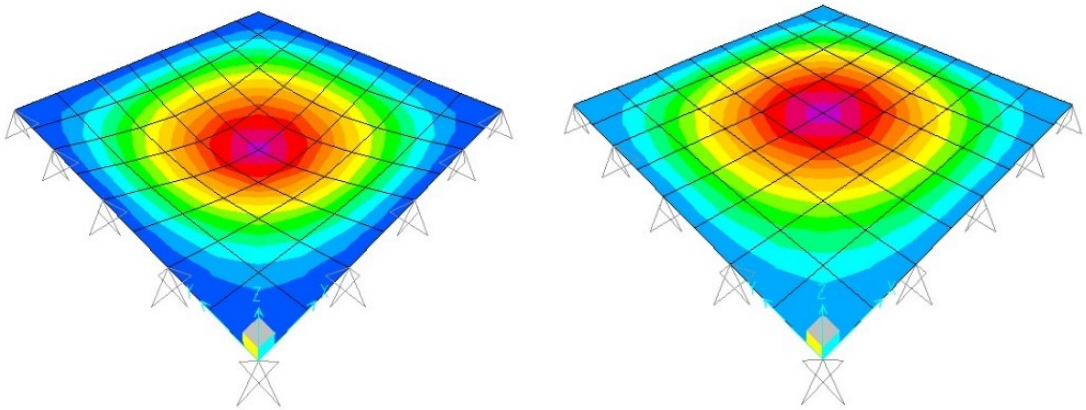

(a) Downward Deflection. **(b)** Upward Deflection.

Fig. 12 Vertical Displacements Obtained from Finite Element.

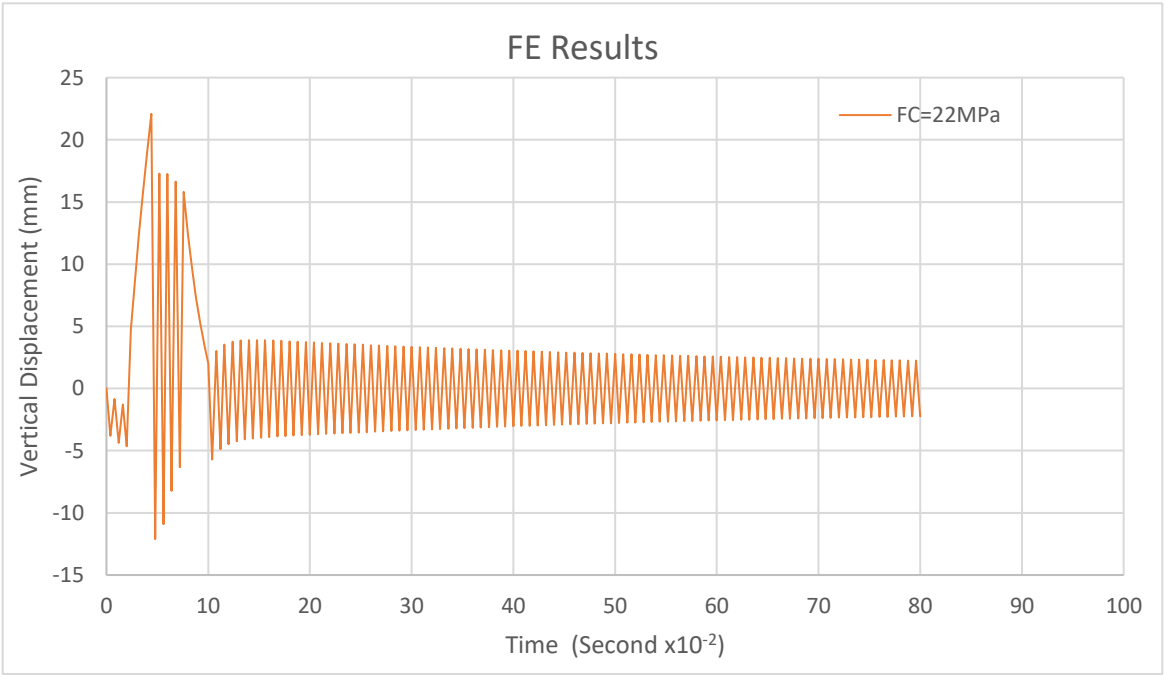

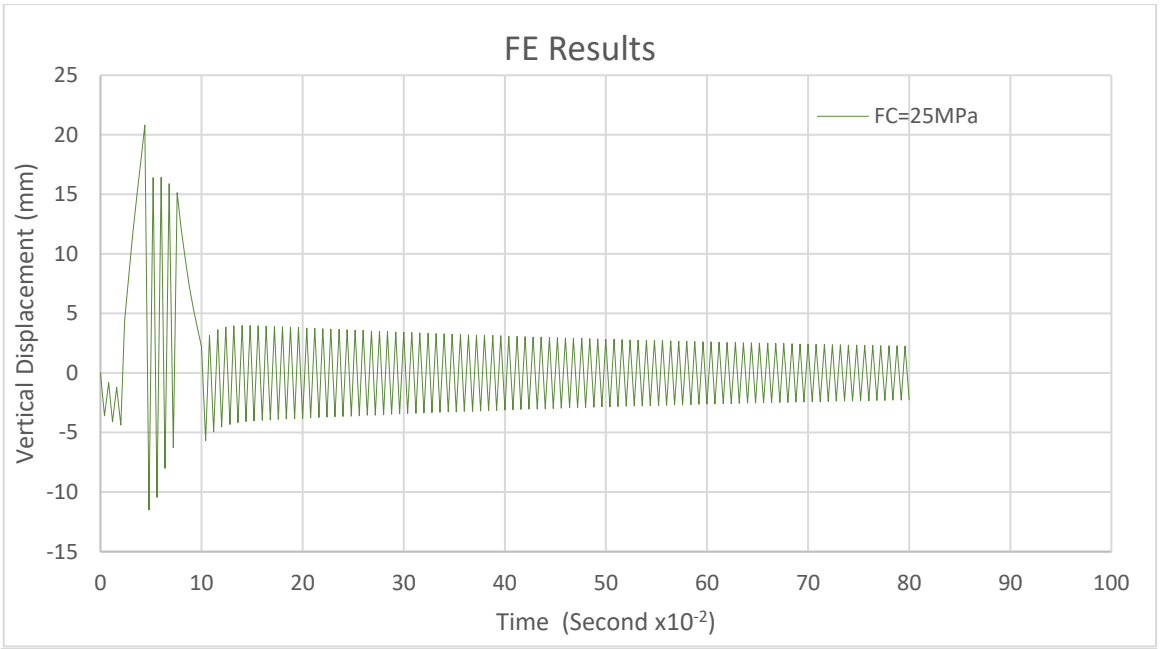

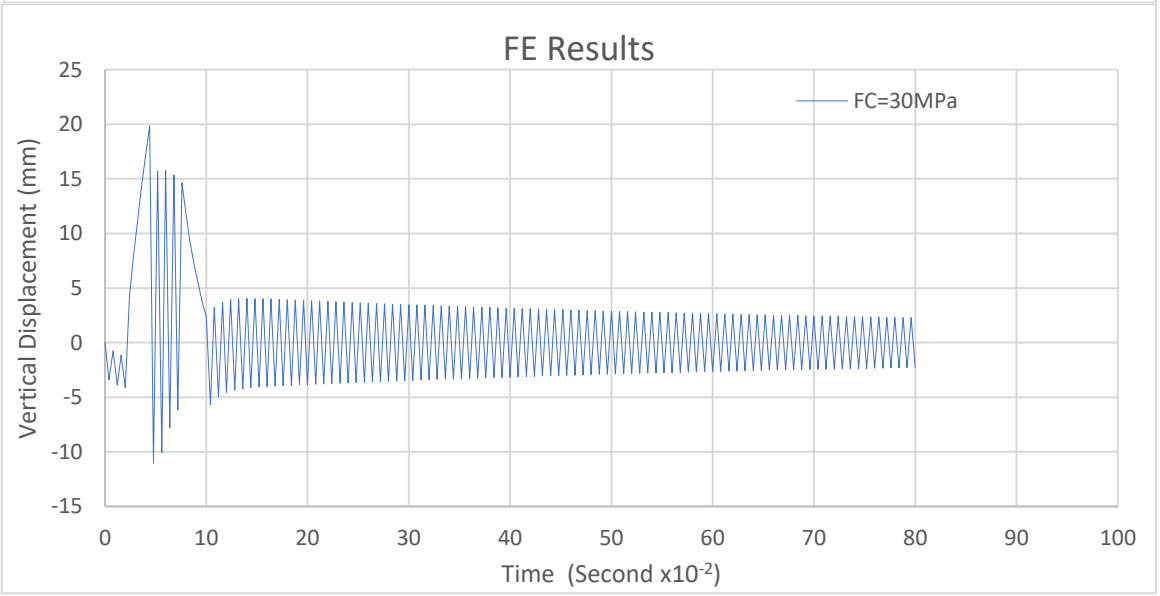

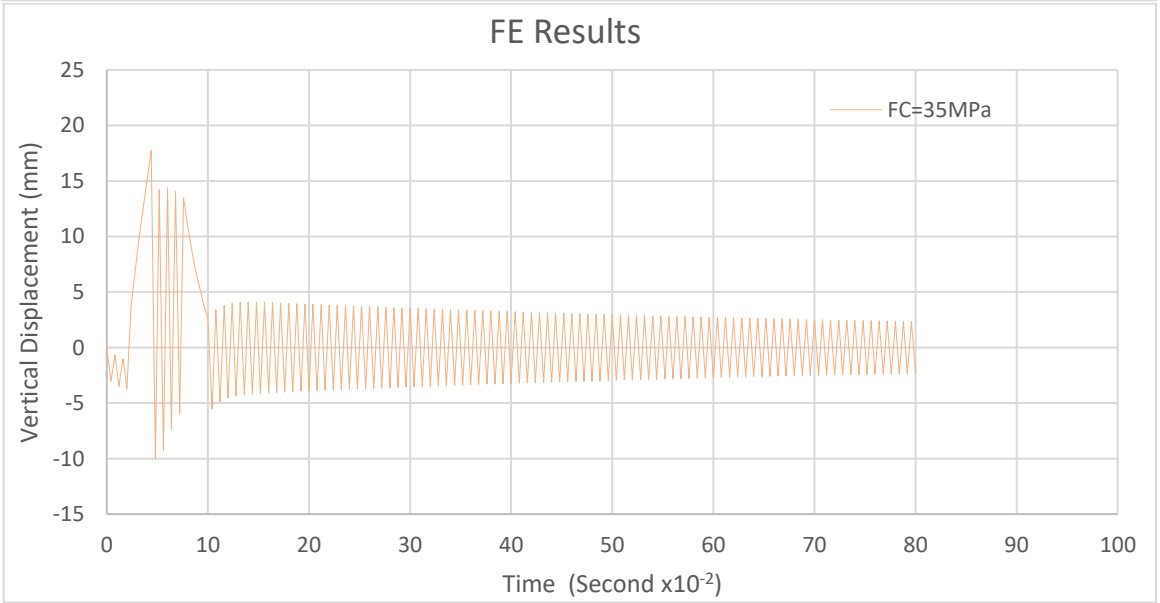

Fig. 13 Vertical Displacements with Time Obtained from Finite Element for Different Concrete Compressive Strength.

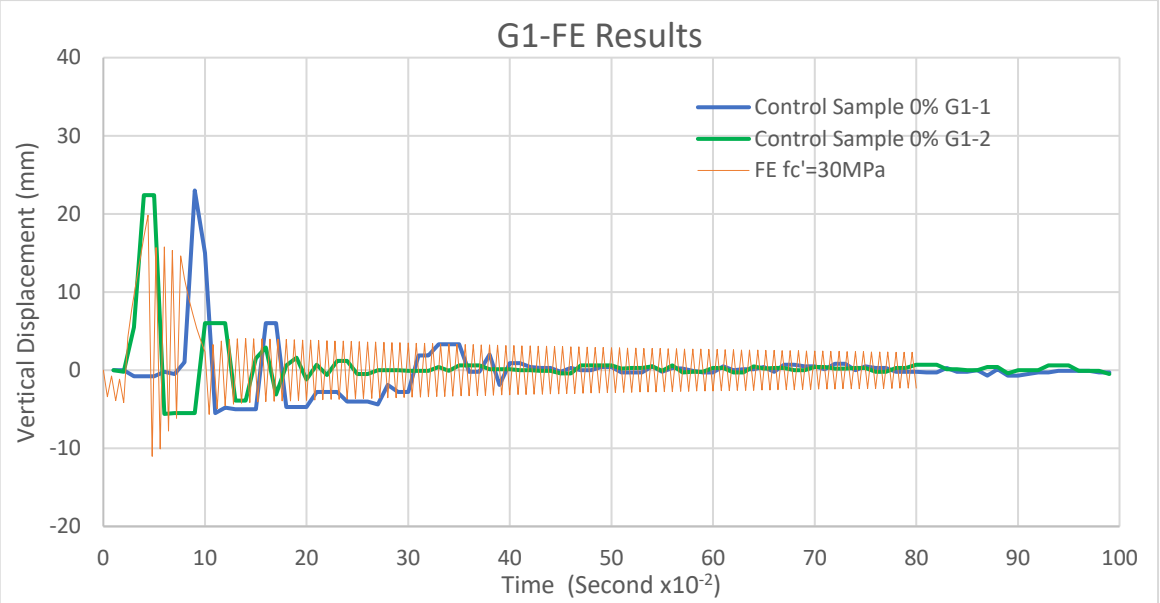
G1-FE Results
Control Sample 0% G1-1
Control Sample 0% G1-2
FE fc'=30MPa
Vertical Displacement (mm)
Time (Second x10-2)

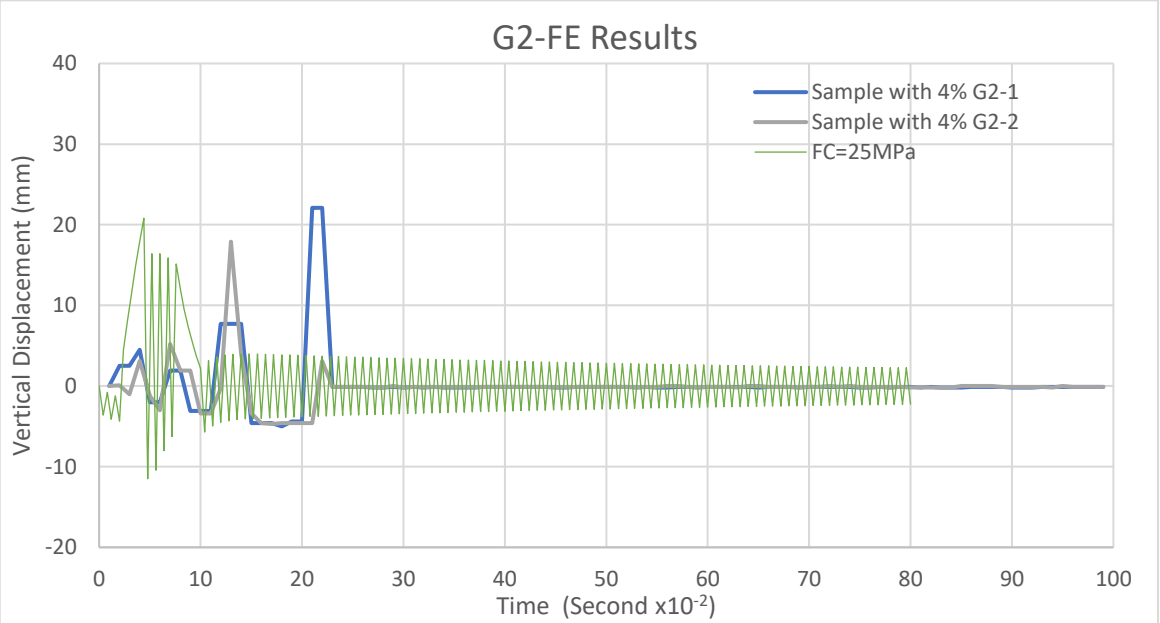
G2-FE Results
Sample with 4% G2-1
Sample with 4% G2-2
FC=25MPa
Vertical Displacement (mm)
Time (Second x10-2)

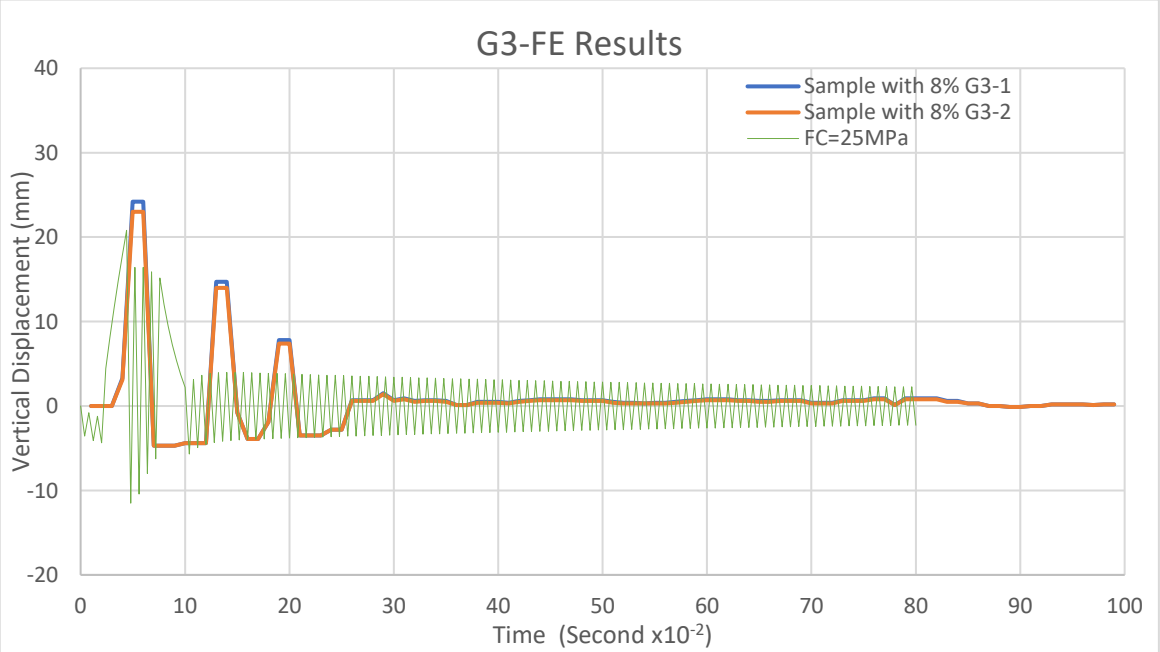
G3-FE Results
Sample with 8% G3-1
Sample with 8% G3-2
FC=25MPa
Vertical Displacement (mm)
Time (Second x10-2)

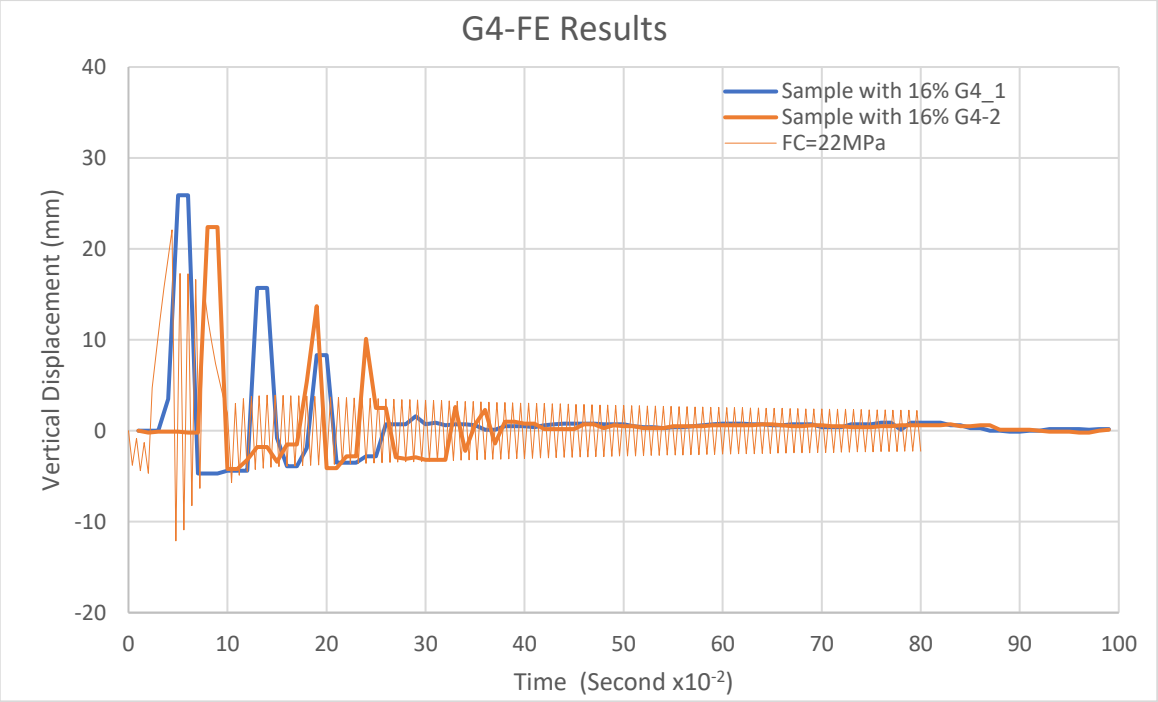

Fig. 14 Vertical Displacements with Time Results from Finite Element and Experimental Results of Group G1.

5.CONCLUSIONS

The investigation's findings showed that:

1) Concrete density was reduced by 2.5% to 9% when replacing the aggregate with shredded PET plastics. In contrast, the fresh concrete' workability increased by about 6% to 16%. Meanwhile, the concrete compressive strength was reduced by about 11.7%, 15.7%, and 19.9% when replacing aggregate by 4%, 8%, and 16% of PET, respectively, compared to normal concrete. The concrete splitting strength was reduced by 7.2%, 17.4%, and 20.3% when replacing aggregate by 4%, 8%, and 16% of PET, respectively, compared to normal concrete.
2) A similar failure behavior was noticed under the impact loads for the four studied groups. Cracking in normal concrete slabs (G1 group) was wider than in concrete with PET plastic slabs (Groups G2, G3, and G4). The PET plastics interaction reduced the cracks developed in the slab under impact load.
3) The partial aggregate replacement by PET in the G2, G3, and G4 groups outperformed the control group G1 regarding impact resistance at first fracture and ultimate failure. Also, the maximal and minimal displacement amplitudes of the slabs with PET decreased with increasing the PET ratio for all groups except G2 (drops 23 and 24) and G3 (in a sporadic fashion). However, they decreased more predictably for the G4 groups.
4) The deflection response obtained from the FE method was almost the same as the response recorded from experiments for all slabs.
5) The finite element program SAP yielded acceptable results when used to model the reinforced concrete slab tested under the impact load. However, deflection obtained by FE was less, about 15.5% and 19%, compared to all groups experimentally tested except slab G2-2, which deflected more than the experimental test results of about 16.3%.
6) The impact energy was increased with the increasing percentage of shredded plastic added to concrete.

ACKNOWLEDGEMENT

The authors appreciate the support they received from the Head of the Civil Engineering Department and the staff of the Materials Laboratory at the University of Mosul's College of Engineering.

REFERENCES

[1] Tahmasebinia F, Tahmasebinia F. **Numerical Modelling of Reinforced Concrete Slabs Subjected to Impact Loading**. M.Sc. Thesis. University of Wollongong; New South Wales, Australia: 2008.

[2] Tahmasebinia F, Remennikov A. **Simulation of the Reinforced Concrete Slabs under Impact Loading**. *Australasian Structural Engineering Conference 2008*; Melbourne, Australia. University of

Wollongong: p. 1–10.

[3] Niza MS. **Computational Analysis of Reinforced Concrete Slabs Subjected to Impact Loads**. *International Journal of Integrated Engineering* 2012; **4**(2): 70–76.

[4] Saatcı S, Batarlar B. **Behavior of Reinforced Concrete Slabs Subjected to Impact Loading**. *10th International Congress on Advances in Civil Engineering 2012*; Ankara, Turkey. Middle East Technical University: p. 1–10.

[5] Batarlar B. **Behavior of Reinforced Concrete Slabs Subjeted to Impact Loads**. M.Sc. Thesis. Izmir Institute of Technology; İzmir, Turkey: 2013.

[6] Teng TL, Chu YA, Chang FA, Chin HS. **Simulation Model of Impact on Reinforced Concrete**. *Cement and Concrete Research* 2004; **34**(11): 2067–2077.

[7] Abdullah ASK. **Impact Behavior of Sandwich Ferrocement Panels**. *Journal of Zankoi Sulaimani Part-A-(Pure and Applied Sciences)* 2016; **18**(3): 1-9.

[8] Li ZC, Jia PC, Jia JY, Wu H, Ma LL. **Impact-Resistant Design of RC Slabs in Nuclear Power Plant Buildings**. *Nuclear Engineering and Technology* 2022; **54**(10): 3745–3765.

[9] Aggestam E, Nielsen JCO, Lundgren K, Zandi K, Ekberg A. **Optimisation of Slab Track Design Considering Dynamic Train–Track Interaction and Environmental Impact**. *Engineering Structures* 2022; **254**: 113749, (1-15).

[10] Kangavar ME, Lokuge W, Manalo A, Karunasena W, Frigione M. **Investigation on the Properties of Concrete with Recycled Polyethylene Terephthalate (PET) Granules as Fine Aggregate Replacement**. *Case Studies in Construction Materials* 2022; **16**: e00934, (1-14).

[11] El-Nadoury WW. **Chemically Treated Plastic Replacing Fine Aggregate in Structural Concrete**. *Frontiers in Materials* 2022; **9**: 948117, (1-11).

[12] Bhutwala AA, Patel HS, Purani VS. **An Investigation on Mechanical Properties of Hybrid Fiber Reinforced Concrete**. *Journal of Emerging Technologies and Innovative Research* 2019; **6**(4): 166–171.

[13] Abdulqadir Z, Mohammed AA. **Impact of Partial Replacement of Ordinary Aggregate by Plastic Waste Aggregate on Fresh Properties of Self-Compacting Concrete**. *Tikrit Journal of Engineering Sciences* 2023; **30**(1):37-53.

[14] Al-Darzi SY. **The Effect of Using Shredded Plastic on the Behavior of Reinforced Concrete Slab**. *Case Studies in Construction Materials* 2022; **17**: e01681, (1-17).

[15] Iucolano F, Liguori B, Caputo D, Colangelo F, Cioffi R. **Recycled Plastic Aggregate in Mortars Composition: Effect on Physical and Mechanical Properties**. *Materials & Design (1980-2015)* 2013; **52**: 916–922.

[16] Alqahtani FK, Zafar I. **Plastic-Based Sustainable Synthetic Aggregate in Green Lightweight Concrete–A Review**. *Construction and Building Materials* 2021; **292**: 123321.

[17] Saxena R, Siddique S, Gupta T, Sharma RK, Chaudhary S. **Impact Resistance and Energy Absorption Capacity of Concrete Containing Plastic Waste**. *Construction and Building Materials* 2018; **10**(176): 415-421.

[18] Hama SM. **Evalutions of Strengths, Impact and Energy Capacity of Two-Way Concrete Slabs Incorprating Waste Plastic**. *Journal of King Saud University-Engineering Sciences* 2021; **33**(5): 337-345.

[19] Hashim S, Khalil A, Sheelan H. **Behavior of Composite Steel Plate-Sustainable Concrete Slabs under Impact Loading**. *Magazine of Civil Engineering* 2021; **6**(106):10604, (1-13).

[20] Mohammed TK, Hama SM. **Mechanical Properties, Impact Resistance and Bond Strength of Green Concrete Incorporating Waste Glass Powder and Waste Fine Plastic Aggregate**. *Innovative Infrastructure Solutions* 2022; **7**(49): 1-12.

[21] Mohammed AA, Karim SH. **Impact Strength and Mechanical Properties of High Strength Concrete Containing PET Waste Fiber**. *Journal of Building Engineering* 2023; **68**: 106195.

[22] Smaoui H, Trabelsi A, Kammoun Z, Aouicha B. **Mechanical, Physical, Blast Waves and Ballistic Impact Resistance Properties of a Concrete Incorporating Thermally Treated PET Inclusions**. *Construction and Building Materials* 2023; **365**: 130088.

[23] Hama SM, Zayan HS, Hama SM. **The Behavior of Concrete Incorporating Ring Shape Waste Plastic Fibers under Different Load Conditions**. *Innovative Infrastructure Solutions* 2023; **8**(5): 134.

[24] Iraqi Specifications, IQS. 5/2018, (2018) Properties of Normal Portland Cement,

National Central Structural Laboratory, 2018: 11.

[25] Iraqi Specification IQS. 45/1984, Aggregate from Natural Sources for Concrete and Construction, National Central Structural Laboratory, 2016: 17.

[26] ASTM C1602/C1602M–06, Standard Specification for Mixing Water Used in the Production of Hydraulic Cement Concrete. ASTM International, West Conshohocken, PA 19428-2959, United States, 2006: 4.

[27] ASTM A615/A615M–15, Standard Specification for Deformed and Plain Carbon-Steel Bars for Concrete Reinforcement, ASTM International, West Conshohocken, PA 19428-2959, United States, 2015: 8.

[28] Neville AM. **Properties of Concrete**. 5th ed., Pearson Education Limited, 2011.

[29] ASTM C138/A138M–01, Standard Test Method for Density (Unit Weight), Yield, and Air Content (Gravimetric) of Concrete, ASTM International, West Conshohocken, PA 19428-2959, United States, 2001: 4.

[30] ASTM C192/C192M–02. Standard Practice for Making and Curing Concrete Test Specimens in the Laboratory, ASTM International, West Conshohocken, PA 19428-2959, United States, 2002: 8.

[31] ASTM C39/C39M–03, Standard Test Method for Compressive Strength of Cylindrical Concrete Specimens, ASTM International, West Conshohocken, PA 19428-2959, United States, 2003: 5.

[32] ASTM C496/C496M–04, Standard Test Method for Splitting Tensile Strength of Cylindrical Concrete Specimens, ASTM International, West Conshohocken, PA 19428-2959, United States, 2004: 5.

[33] Reda Taha MM, El-Dieb AS, Abd El-Wahab MA, Abdel-Hameed ME. Mechanical, fracture, and microstructural investigations of rubber concrete. *Journal of Materials in Civil Engineering* 2008; **20**(10): 640–649.

[34] Hibbeler RC. **Engineering Mechanics: Dynamics**. 14th ed., New Jersey, USA: Pearson Educación, 2016.

[35] Shukur MH, Ibrahim KA, Al-Darzi SY, Salih OA. **Mechanical Properties of Concrete Using Different Types of Recycled Plastic as an Aggregate Replacement**. *Cogent Engineering* 2023; **10**(1):2243735, (1-21).

[36] CSI Committee. CSI Analysis Reference Manual for SAP2000, ETABS, and SAFE, Computer and Structures Inc.; Berkeley, California, USA, 2009.

[37] Chapelle D, Bathe KJ. **The Finite Element Analysis of Shells-Fundamentals**. 2nd ed., New York: Springer Science & Business Media; 2010.

[38] ACI Committee 318. Building Code Requirements for Structural Concrete (ACI318-19), American Concrete Institute, Farmington Hills, USA, 2019: 1253.